Biosensors

AFM-Tip-Integrated Amperometric Microbiosensors: High-Resolution Imaging of Membrane Transport**

Angelika Kueng, Christine Kranz, Alois Lugstein, Emmerich Bertagnolli, and Boris Mizaikoff*

The mapping of molecular transport across membranes at the single-cell level is one of the major challenges in cell physiology. Miniaturized biosensors offer many advantages by combining the selectivity of biological recognition with well-established principles of transduction. To date, the combination of biosensing with atomic force microscopy (AFM) is mainly based on the mass-sensitive detection of binding events that change the deflection of a cantilever which is surface-modified with immobilized bioreceptors. Many biochemically relevant processes are based on the electrochemical conversion of molecules; therefore, techniques for obtaining laterally resolved information on coupled oxidation–reduction processes with correlation in space and time are of particular interest.[1] Scanning electrochemical microscopy (SECM) has proven to be a versatile tool for spatially resolved measurements of molecular transport across porous membranes.[2–4] Spatially resolved electrochemical information on interface processes is provided by combining electroanalytical techniques with the principle of scanning a microelectrode in close vicinity across the sample surface.[5] Few applications of miniaturized scanning biosensors combined with SECM are described in the literature.[6,7] A main limitation is the achievable lateral resolution, which is not comparable to that of AFM or consistent with the targeted imaging of membrane-transport processes at a molecular level.

A major step toward overcoming these limitations was recently made with the integration of micro- and nanoelectrodes into AFM tips.[8,9] An electroactive area with defined geometry, which is recessed from the apex of an AFM tip (Figure 1a and b), allows integration of SECM[10–12] functionality into AFM by correlating the current measured at the integrated electrode with the topographical information obtained by the AFM tip. These combined AFM–SECM probes retain the integrity of both techniques, and can be applied in dynamic-mode operation at soft biological samples.[13]

Herein, well-established protocols for the immobilization of biological recognition elements, such as enzymes, are applied to integrate micro- and nanobiosensors into AFM tips. The defined electrode geometry and the employed immobilization techniques result in a confined immobilization of the biological recognition element at the electrode surface. Enzymatic conversion of electroactive and -inactive species generated at the sample surface is possible by the immobilization of enzymes through self-assembled thiol monolayers with reactive headgroups[14] (Figure 1b(B)) or polymer-film entrapment[15,16] (Figure 1b(A)). Hence, simultaneous imaging of surface morphology and biologically relevant analytes involved in surface processes significantly extends the applicability of this technology. This integrated approach, along with the high sensitivity and fast response time of amperometric micro- and nanobiosensors, provides the spatial and temporal resolution for the investigation of cellular processes at the nanometer scale.

A synthetic model was selected to mimic glucose transport through cellular membranes. The high-resolution mapping of glucose membrane transport was carried out by immobilizing glucose oxidase at the surface of the AFM-tip-integrated electrode by electrochemically induced, localized precipitation of enzyme-containing polymer suspensions.[15] Glucose biosensors fabricated with this technology exhibit excellent sensitivity, response time, reproducibility, and long-term stability.

Figure 1c shows a schematic representation of the imaging mode for laterally resolved mapping of glucose membrane

[*] Dr. A. Kueng, Dr. C. Kranz, Prof. Dr. B. Mizaikoff
School of Chemistry and Biochemistry
Georgia Institute of Technology
Atlanta, GA 30332-0400 (USA)
Fax: (+1) 404-385-6447
E-mail: christine.kranz@chemistry.gatech.edu
Dr. A. Lugstein, Prof. Dr. E. Bertagnolli
Solid State Electronics Institute
Vienna University of Technology
Floragasse 7, 1040 Vienna (Austria)

[**] This work is supported by NSF (grant 0216368) within the program "Biocomplexity in the Environment", the National Institute of Health (grant EB000508), and the "Fonds zur Förderung der wissenschaftlichen Forschung" Austria (grants P14122-CHE and J2230). PCT patent on this technology: WO0194877A1.

 DOI: 10.1002/ange.200461556

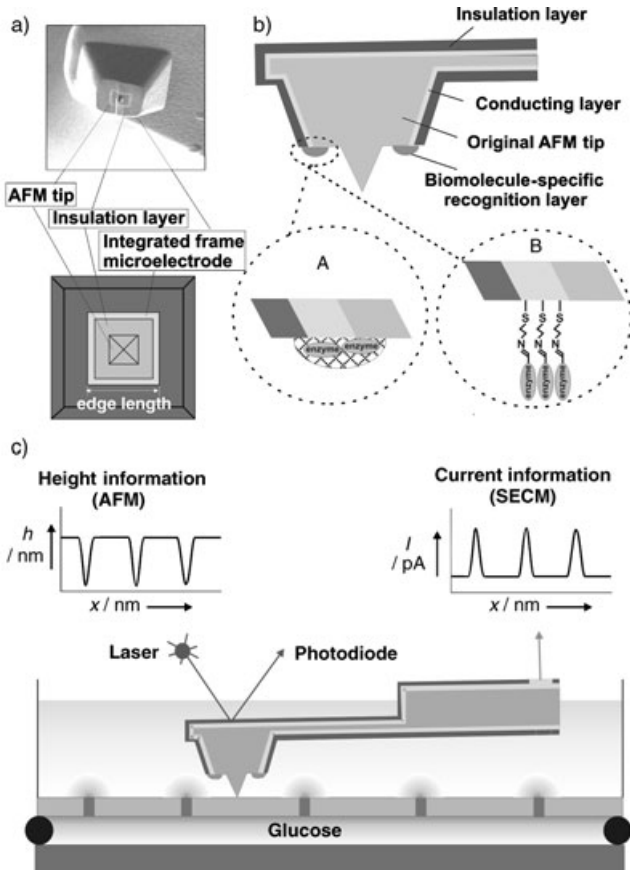

Figure 1. a) SEM image and schematic top view of an AFM-tip-integrated frame electrode; b) schematic cross section of an AFM-tip-integrated biosensor. Enzymes can be immobilized at the surface of the scanning-probe tip-integrated electrode through self-assembled thiol monolayers with functionalized headgroups (A) or through electrochemical deposition of enzyme-containing polymer films (B). c) Schematic cross section of the experimental setup for imaging glucose transport through a porous membrane during simultaneous AFM mapping.

transport with AFM-tip-integrated glucose biosensors. Images were recorded in AFM dynamic mode,[17] a prerequisite for the investigation of soft biological samples, and in SECM generation/collection (G/C) mode.[12] In G/C operation, the current response arises from an electroactive species generated at the sample surface. The integrated electrode or microbiosensor acts as a sensor that establishes concentration profiles of individual species near the sample surface. The signal traces in Figure 1c schematically illustrate schematically the expected qualitative height and current signals recorded with the bifunctional probe scanned in the x direction above a synthetic membrane with 200-nm pores. As the reshaped AFM tip is imaging the pores, which corresponds to a decrease in the height signal, glucose is diffusing through the pores toward the immobilized glucose oxidase layer, which catalyzes the conversion of glucose into gluconolactone. The corresponding reactions are summarized in Figure 2a. The resulting current measured at the integrated electrode arises from the oxidation of the enzymatically generated by-product H_2O_2, which is oxidized at the electrode surface at a bias voltage of 650 mV versus Ag/AgCl. Therefore, the current signal increases during imaging of the pores as a result of glucose diffusion from the donor into the receptor compartment.

Prior to application, the AFM-tip-integrated enzyme electrodes were characterized in an electrochemical cell by constant-potential amperometry. The calibration function obtained for the AFM-tip-integrated glucose biosensor is shown in Figure 2b and exhibits adequate linearity with an R^2 value of 0.9889 in the concentration range of 0.5–2.5 mM glucose in aqueous solution.

Simultaneously recorded AFM topography (Figure 2c) and SECM current images in the presence (Figure 2d) and absence (Figure 2f) of glucose in the donor compartment, and exemplary line scans of the height and current response (Figure 2e) are also presented. The current recorded at the AFM-tip-integrated glucose biosensor during the imaging of the pores increases as a result of the localized production of H_2O_2. The glucose signal response in the electrochemical image corresponds to the topography measured simultaneously with the AFM tip. The SECM current image of the porous membrane represents a contour map of the glucose concentration after emergence of the aqueous solution of

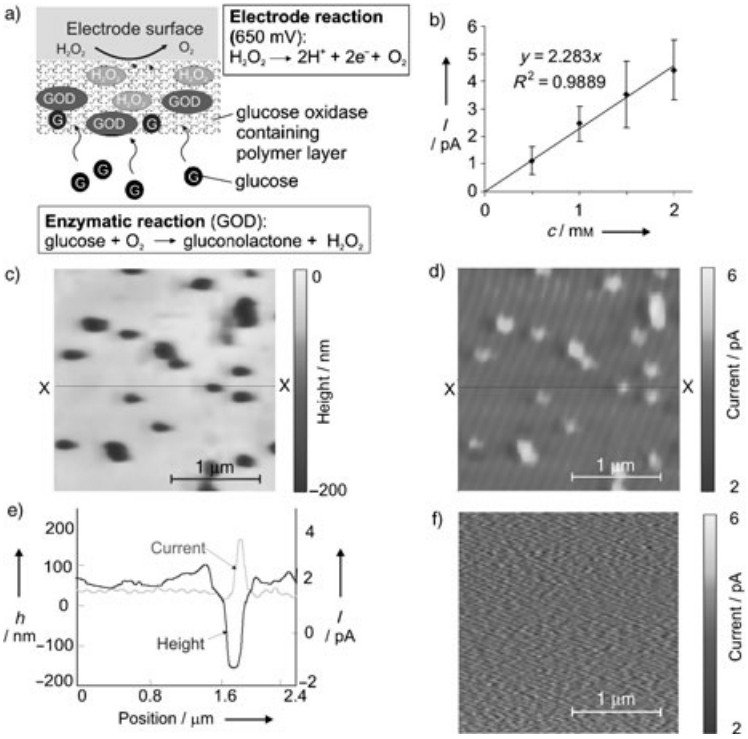

Figure 2. a) Reactions for glucose detection with a biosensor based on glucose oxidase (GOD). b) Glucose calibration of an AFM-tip-integrated biosensor (edge length: 800 nm) fabricated by entrapment of glucose oxidase within a polymer film. Simultaneously recorded c) height and d) current images of glucose diffusion through a porous polycarbonate membrane (pore size: 200 nm); images recorded in AFM dynamic mode. e) Exemplary corresponding line scans of height and current. f) Current image recorded without glucose in the donor compartment.

glucose from the membrane pore and free diffusion into the receptor-compartment solution. As is evident in the control experiment, the measured current is negligible without glucose in the donor compartment (Figure 2 f).

Quantification of the current signal obtained requires precise knowledge of the electrode geometry and the absolute distance between the electrochemical probe and the sample surface, which is provided by the bifunctional AFM–SECM probes. Furthermore, by applying a simple single-pore model previously described for the analysis of SECM images at membranes,[2,18] the flux of glucose away from the pore opening is assumed to be dominated by radial diffusion in the absence of an appreciable convective flow. The glucose transport rate can be obtained by assuming that the pore opening is hemispherical and solving the continuity equation by using Fick's law at appropriate boundary conditions.[19–22]

The concentration profile $C(r)$ at a radius r above the hemispherical pore opening can be described by Equation (1), where C_S represents the concentration of the molecule at the surface of the pore opening. Earlier results demonstrated that the radial divergence of the diffusive flux from a microscopic pore, regardless of its real shape, results in the pore appearing as if it were hemispherical in shape.[19] For a disk-shaped pore with radius a, the radius of the corresponding hemispherical pore r_0 can be described by Equation (2).

$$C(r) = (r_0/r)C_S \quad (1)$$

$$r_0 = 2a/\pi \quad (2)$$

On the basis of this approach, the theoretical glucose concentration at a distance (r) of 310 nm, which corresponds to the reshaped AFM tip height, above a pore opening with a radius of 100 nm (a) is estimated to be 0.62 mM for a 3 mM glucose solution. The evaluation of the current response in the SECM image (Figure 2 d) results in an average peak current of 1.5 ± 0.3 pA. According to the linear regression of the glucose calibration obtained at the AFM-tip-integrated electrode (Figure 2 b), the measured glucose concentration is estimated to be 0.66 ± 0.13 mM. This semiquantitative value corresponds well to the theoretically estimated concentration of 0.62 mM.

To demonstrate the versatility of the proposed technique for a wider range of applications, horseradish peroxidase (HRP) was immobilized at the surface of an AFM-tip-integrated electrode through self-assembled thiol monolayers with reactive headgroups (Figure 1 b (B)).[14] Simultaneously recorded topographical (AFM-tip) and electrochemical (substrate-generated) images were obtained by immobilizing a peroxidase layer at the surface of an AFM-tip-integrated electrode. The reactions involved are shown schematically in Figure 3. The peroxidase activity was imaged in the tip-generation/substrate-collection mode of SECM (see Figure 3 a) during AFM contact-mode operation. At the AFM-tip-integrated electrode, the enzyme-catalyzed reduction of H_2O_2 involves ferrocene methanol (Fc) as an electron donor. Ferrocenium methanol (Fc^+, which contains Fe^{2+}), the electroactive by-product of the HRP-catalyzed reaction,

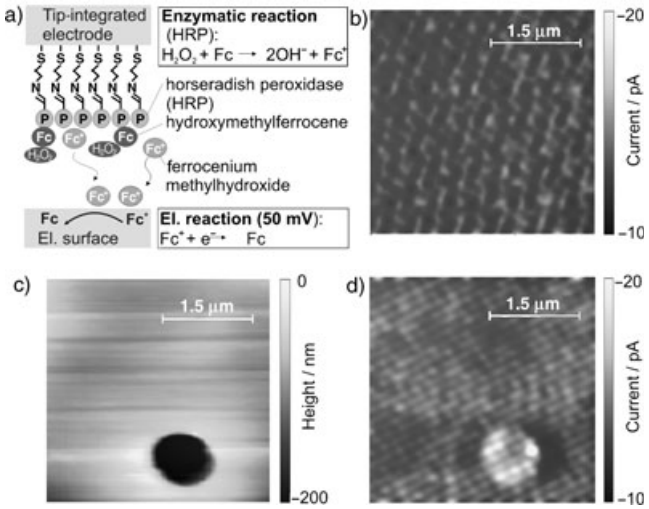

Figure 3. a) Reactions and detection scheme of the experiment in the tip-generation/substrate-collection mode for imaging with an AFM-tip-integrated biosensor based on horseradish peroxidase (HRP). Topographical information and tip-integrated peroxidase activity is recorded simultaneously by contact-mode AFM operation. The current measured at the microelectrode array reflects the enzyme activity of the HRP biosensor integrated into the AFM tip. Top view of the height (c) and simultaneously recorded current in the presence (d) and absence (b) of H_2O_2 in solution. El. = electrode.

diffuses to the biased sample surface, which comprises a microstructured electrode array where Fc^+ is reduced at a selected potential not amenable to any other species in solution. The simultaneously obtained topography of an individual microstructured disk electrode and the local (electro)chemical activity are shown in Figure 3 c and 3 d, respectively. Comparison with the control experiment in the absence of H_2O_2 (Figure 3 b) demonstrates the successful application of tip-integrated enzyme layers in bifunctional SECM–AFM probes for SECM tip generation/substrate collection.

AFM-tip-integrated imaging biosensors are a promising concept that combine the advantages of high selectivity provided by amperometric microbiosensors with high-resolution scanning probe microscopy based on microfabricated multifuntional scanning probes. High reproducibility of the fabrication process and the size of the integrated sensors in the micro- to nanodomain make them a versatile tool for future applications in probing a wide range of biologically relevant processes at a cellular level. The presented technology provides a concept for the simultaneous detection of surface morphology and (electro)chemical activity with high selectivity and high lateral resolution, on the basis of this concept of "imaging nanobiosensors". Accurate positioning and scanning of nanobiosensors at a defined distance above the sample surface provides quantitative kinetic parameters with high lateral and temporal resolution. Given the flexibility of the technology, there is considerable scope for the extended use of multifunctional scanning probes for a wide range of biological specimens and processes.

Experimental Section

AFM-tip-integrated gold electrodes (thickness of the gold layer: 100 nm, parylene C insulation layer: 800 nm) were fabricated and characterized as previously described.[8,9] All measurements were carried out with a Pico Plus AFM (Molecular Imaging, Tempe, AZ). The output signal of the bipotentiostat (A-832, CH Instruments, Austin, TX) was read at an additional AD/DA channel offered by the AFM instrument. The faradaic current recorded at the integrated electrode was obtained simultaneously with the topographical information provided by the reshaped AFM tip.

Imaging of glucose membrane transport with an AFM-tip-integrated biosensor based on glucose oxidase: The AFM–SECM tip used for imaging glucose diffusion through the synthetic porous membrane had an edge length of 800 nm and a reshaped tip height of 310 nm. Selective electrode-surface modification was performed by the pH-shift-induced polymerization of enzyme-containing films.[15] For polymer-film formation, a potential-pulse profile (2200 mV for 0.2 s, 800 mV for 1 s, and 0 mV for 5 s versus Ag/AgCl) was applied for one cycle, which led to the formation of an enzyme-containing polymer layer selectively deposited on the electrode surface.

Calibration of the tip-integrated biosensor was carried out by constant-potential amperometry by using a bipotentiostat (A832, CH Instruments, Austin, TX) and an electrochemical cell equipped with a Pt counter electrode and an Ag/AgCl reference electrode containing 10 mL of phosphate-buffered saline (PBS) solution at pH 7.4. The enzyme-modified electrode was operated at a potential of 650 mV versus Ag/AgCl to oxidize the H_2O_2 formed during the reaction catalyzed by glucose oxidase. After the current signal reached a steady-state value, aliquots of a glucose standard solution (0.2 M) were injected and the increase in current was monitored.

To study glucose membrane transport, a porous polycarbonate membrane (200-nm pore size, Osmonics Inc., Minnetonka, MN) was mounted in a custom-built vertical diffusion cell that separated aqueous solutions in the donor and receptor compartments (see Figure 1c). Measurements were performed in PBS solution (pH 7.4). The donor solution (bottom) contained glucose (3 mM). All measurements were carried out in a three-electrode setup with an Ag/AgCl reference electrode and a platinum-wire counter electrode at room temperature. The integrated biosensor was biased at a potential of 650 mV to oxidize evolving H_2O_2. Scan area: 2450×2450 nm, scan rate: 1 line s^{-1}, drive frequency: 32 kHz, tip potential: 650 mV versus Ag/AgCl.

Imaging with an AFM-tip integrated biosensor based on horseradish peroxidase: The AFM–SECM tip (edge length: 860 nm, tip height: 410 nm) was cleaned in H_2SO_4/H_2O_2 (70:30 v/v) for 30 s, rinsed three times with water, and then immediately immersed in cystaminium dichloride (0.1 M in acetate buffer; pH 5.5) for 30 min. After rinsing the probe five times with deionized water, HRP (1 mg) in phosphate buffer (100 μL, pH 7.0) containing 2.5% (v/v) glutaraldehyde was immobilized on the integrated gold electrode for 2 h. The probe was thoroughly rinsed with buffer solution several times, and the sample was stored at 4 °C prior to use.

The AFM–SECM experiment was carried out in AFM contact and SECM tip-generation/substrate-collection modes in ferrocene methanol (Fc, 2 mmol) in phosphate buffer (0.1 M, pH 7.0) with KCl (0.1 M) as the electrolyte in the presence and absence of the enzymatic substrate H_2O_2 (0.5 mmol). The microstructured gold sample (Quantifoil Micro Tools, Jena, Germany) was biased at a potential of 50 mV versus Ag/AgCl to reduce ferrocenium methanol (Fc^+). Scan area: 4×4 μm, scan rate: 1 line s^{-1}.

Received: August 5, 2004
Revised: February 28, 2005
Published online: April 28, 2005

Keywords: biosensors · glucose · membranes · scanning probe microscopy

[1] J. K. H. Horber, M. J. Miles, *Science* **2003**, *302*, 1002.
[2] B. D. Bath, H. S. White, E. R. Scott, *Scanning Electron Microsc.* **2001**, 343.
[3] O. D. Uitto, H. S. White, K. Aoki, *Anal. Chem.* **2002**, *74*, 6131.
[4] B. D. Bath, R. D. Lee, H. S. White, E. R. Scott, *Anal. Chem.* **1998**, *70*, 1047.
[5] A. J. Bard, F. R. F. Fan, D. T. Pierce, P. R. Unwin, D. O. Wipf, F. Zhou, *Science* **1991**, *254*, 68.
[6] A. Hengstenberg, C. Kranz, W. Schuhmann, *Chem. Eur. J.* **2000**, *6*, 1547.
[7] B. R. Horrocks, D. Schmidtke, A. Heller, A. J. Bard, *Anal. Chem.* **1993**, *65*, 3605.
[8] C. Kranz, G. Friedbacher, B. Mizaikoff, A. Lugstein, J. Smoliner, E. Bertagnolli, *Anal. Chem.* **2001**, *73*, 2491.
[9] A. Lugstein, E. Bertagnolli, C. Kranz, A. Kueng, B. Mizaikoff, *Appl. Phys. Lett.* **2002**, *81*, 349.
[10] R. C. Engstrom, M. Weber, D. J. Wunder, R. Burgess, S. Winquist, *Anal. Chem.* **1986**, *58*, 844.
[11] R. C. Engstrom, T. Meaney, R. Tople, R. M. Wightman, *Anal. Chem.* **1987**, *59*, 2005.
[12] C. Lee, J. Kwak, F. C. Anson, *Anal. Chem.* **1991**, *63*, 1501.
[13] A. Kueng, C. Kranz, A. Lugstein, E. Bertagnolli, B. Mizaikoff, *Angew. Chem.* **2003**, *115*, 3358; *Angew. Chem. Int. Ed.* **2003**, *42*, 3238.
[14] T. Wilhelm, G. Wittstock, R. Szargan, *Fresenius J. Anal. Chem.* **1999**, *365*, 163.
[15] C. Kurzawa, A. Hengstenberg, W. Schuhmann, *Anal. Chem.* **2002**, *74*, 355.
[16] A. Kueng, C. Kranz, B. Mizaikoff, *Biosens. Bioelectron.* **2004**, *19*, 1301.
[17] P. K. Hansma, J. P. Cleveland, M. Radmacher, D. A. Walters, P. E. Hillner, M. Bezanilla, M. Fritz, D. Vie, H. G. Hansma, C. B. Prater, J. Massie, L. Fukunaga, J. Gurley, V. Eilings, *Appl. Phys. Lett.* **1994**, *64*, 1738.
[18] A. Kueng, C. Kranz, B. Mizaikoff, *Biosens. Bioelectron.* **2004**, in press; published in ASAP section.
[19] E. R. Scott, H. S. White, J. B. Phipps, *Anal. Chem.* **1993**, *65*, 1537.
[20] J. Crank, *The Mathematics of Diffusion*, Oxford University Press, New York, **1956**.
[21] E. L. Cussler, *Diffusion: Mass Transfer in Fluid Systems*, Cambridge University Press, New York, **1997**.
[22] A. J. Bard, L. R. Faulkner, *Electrochemical Methods*, Wiley, New York, **1980**.

